Finite-Size Effects in the Conductivity of Cluster Assembled Nanostructures

J. Schmelzer, Jr.,* S. A. Brown,† A. Wurl, and M. Hyslop

Nanostructure Engineering Science and Technology (NEST) Group and Department of Physics & Astronomy, University of Canterbury, Christchurch, New Zealand

R. J. Blaikie

Nanostructure Engineering Science and Technology (NEST) Group and Department of Electrical & Electronic Engineering, University of Canterbury, Christchurch, New Zealand

(Received 5 November 2001; published 17 May 2002)

Atomic clusters have been deposited between lithographically defined contacts with nanometer scale separations. The design of the contacts is based on an appropriate application of percolation theory to conduction in cluster deposited devices and allows finite-size effects to be clearly observed. It is demonstrated, both by experiment and by simulation, that for small contact separations the percolation threshold is shifted to extremely low surface coverages. The selected rectangular contact geometry ensures that wirelike structures are formed close to the percolation threshold.

DOI: 10.1103/PhysRevLett.88.226802 PACS numbers: 73.63.–b, 36.40.–c, 64.60.Ak, 81.07.–b

Atomic clusters are nanoscale particles that bridge the gap between atoms/molecules and condensed matter and exhibit a range of unusual structural, electronic, and other properties [1–4]. While these unusual properties are sometimes "remembered" even in macroscopic cluster assembled films [4], there have been relatively few attempts to take advantage of the novel functionality of clusters by incorporating them in nanoscale devices (see, for example, [5–10]), and exploration of new, simple, low-cost fabrication methods is highly desirable. In addition to "memory effects," suitable cluster assembled nanostructures will exhibit distinctive properties that arise from the small overall system size (i.e., "finite-size effects" [11]). The range of film parameters that can be controlled—cluster material, size of cluster, and overall system size—therefore offers new opportunities [3,12,13] for engineering nanoelectronic devices whose properties might eventually be governed by the unusual properties of the clusters. In this work we begin an exploration of the possibility of nanodevice fabrication using a straightforward cluster deposition technique that avoids laborious manipulation of the clusters. We focus on the use of relatively large Bi clusters to investigate finite-size effects and the formation of cluster assembled nanowires close to the percolation threshold.

A simple model of a cluster deposited film is a two-dimensional square lattice where a random fraction p ($0 < p < 1$) of the available lattice sites is occupied. The number, size, and shape of the connected structures are described by percolation theory [14]: in an infinite system the structures generated by connecting neighboring occupied lattice sites will be small and isolated for $p < p_C$ and form an infinite network for $p > p_C$, where $p_C = 0.592\,746\,1$ is the percolation threshold. At the critical coverage p_C a geometrical second order phase transition occurs with power laws and corresponding critical exponents describing the behavior of quantities such as the correlation length, probability of a site belonging to the infinite network, and conductivity. According to the universality hypothesis [15], the critical exponents depend only on a few fundamental properties of the respective model (dimension, kind of interaction) and therefore estimates for the critical exponents obtained from very simple models can apply to more complex or experimental systems [16].

In this study we investigate the conductivity of a cluster deposited film with nanoscale overall dimensions (300 to 3200 nm); however, it is important to first discuss a percolation model which facilitates an understanding of the design of the experiments and of the experimental results. We consider rectangular samples with separation between the contacts L and width of the contacts $w \gg L$ (L and w measured in lattice spacings). The contacts are attached to the long sides of the rectangle so, e.g., for $L = 5$ only five lattice sites fit between the contacts. Rectangular rather than square arrays have been studied because of the stochastic nature of the process under consideration. For small systems, statistical fluctuations become increasingly significant and so an estimate of the expectation value for any quantity can be obtained only by averaging over many independent samples. While averaging over a large number of square samples is possible in simulations, it is impractical in experiments due to time limitations and the difficulty in producing identical experimental conditions over a large number of runs. Our rectangular structures, however, intrinsically average over w/L squares, allowing the collection of data with small statistical error in a single deposition. More importantly, the rectangular structures allow the unambiguous observation of the effect of the finite system size on the onset of conduction. The rectangular geometry also ensures that in each device the first connection between the contacts is formed by a member of the ensemble of square arrays which creates a more or less direct path between the contacts.

The simple site percolation model can be used to calculate the conductivity of a network by assigning resistances to each occupied lattice site. Figure 1 shows results of computer simulations of the conductivity σ (normalized per unit square) as a function of coverage p and contact separation L (for large w). *Finite-size effects in the conductivity are very pronounced;* i.e., for smaller contact separations conduction occurs at a much lower coverage. Finite-size scaling theory [14] suggests that all finite-size deviations can be accounted for by the following scaling ansatz:

$$\sigma(p,L) = L^{-t/\nu} f_\sigma[(p - p_C)L^{1/\nu}], \qquad (1)$$

and this is indeed the case for the data in Fig. 1 (f_σ is a suitable scaling function, t is the critical exponent for the conductivity, and ν is the critical exponent for the correlation length).

To allow comparison with our experiments, we define the effective percolation threshold $p_{\text{onset}}(L)$ to be the coverage at which the conductivity reaches some value σ_{min}, which could be viewed as the minimum conductivity measurable by the ammeter. The effective percolation threshold then depends on the choice of σ_{min} as well as the system size L, as illustrated in Fig. 1. Using Eq. (1), it can be shown that in the limit of small σ_{min}, a scaling relation of the form

$$p_{\text{onset}} - p_C \propto L^{-z} \qquad (2)$$

holds, with $z = 1/\nu$ (where $\nu = 4/3$ for two-dimensional lattices). The simulational results can be used to confirm Eq. (2) by calculating the exponent z as a function of σ_{min}. In contrast to the conventional definition of the percolation threshold for a $L \times w$ system, where $z = 1/\nu$ always [14,17], Fig. 2 shows that for our definition of the percolation threshold $z = 1/\nu$ only as $\sigma_{\text{min}} \to 0$. In our experiments σ_{min} is very small ($<10^{-6}$) and so, for $p < p_{\text{onset}}$, the measured conductivity is also small (determined by leakage and noise). At the percolation threshold the conductivity jumps to a value σ^*_{min}, which is calculated to be $\sim 10^{-3}$ in the geometry of our experiments.

To summarize, we have shown that the dependence of the effective percolation threshold p_{onset} on system size L should allow the deduction of the exponent for the correlation length, ν, from experimental conductivity measurements. Equation (2) represents a well-defined prediction of how the effective percolation threshold scales with system size and therefore forms the basis of an understanding of the cluster deposition experiments. Most importantly, the simulations suggest that conducting paths can be formed *at low surface coverages* by using rectangular contacts with small separations: in this regime there must be a wirelike path between the contacts.

In the experiment a beam of bismuth clusters with a mean diameter of (60 ± 10) nm is generated in an inert-gas aggregation source [3]. Deposition onto a substrate with prefabricated contacts is controlled by a shutter. The NiCr/Au contacts are defined on highly insulating and flat surfaces of a 200 nm SiN layer grown on a Si wafer, using a combination of standard optical and electron beam lithography (EBL) techniques. Figure 3 shows optical microscope images of a sample with two pairs of contacts, prior to deposition. The interdigitated contacts allow for a high w/L ratio in a compact area. Atomic force microscopy (AFM) has been used to measure accurately the contact separations (ranging from 300 to 3200 nm) and also to characterize contactless, large-area samples consisting of cluster films deposited onto 3 mm × 3 mm pieces of SiN. AFM images of the latter films, with a wide range of coverages (examples are shown in Fig. 4), clearly show that the bismuth clusters stick to the SiN surface on landing and do not diffuse and aggregate to form larger particles.

During deposition a dc bias of 1.2 V is applied across the contacts and the current is measured as a function of

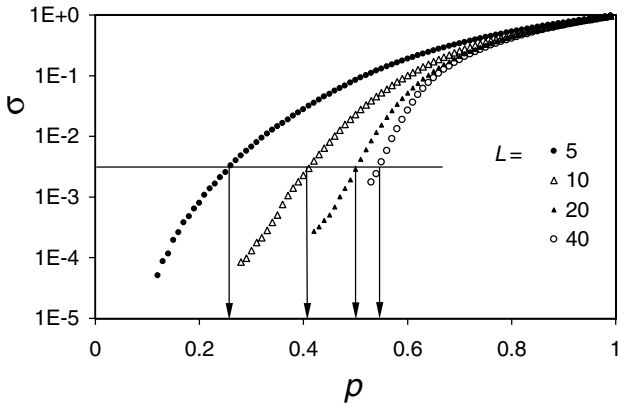

FIG. 1. Normalized conductivity as a function of p for four different system sizes L; the horizontal line indicates a particular choice of minimum observable conductivity σ_{min} and the arrows point to the corresponding p_{onset} values for each system size as described in the main text.

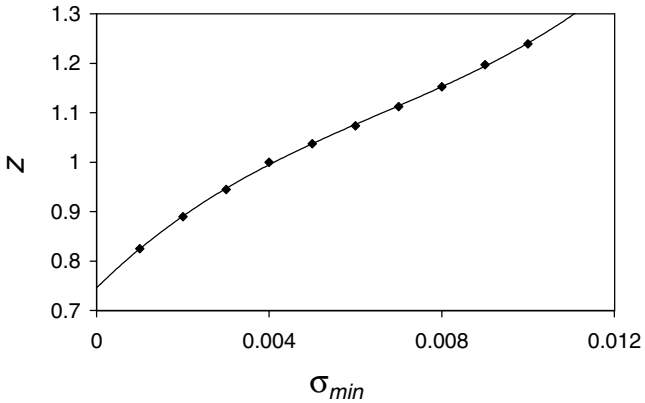

FIG. 2. Scaling exponent z for the effective percolation threshold $p_{\text{onset}}(L)$ as a function of the minimum observable conductivity σ_{min} [see Eq. (2)]. The solid line is a third order polynomial fit to the data: the fit intercepts the vertical axis at $z = 0.746 \pm 0.006$ which is consistent with the expected critical exponent $1/\nu = 0.75$.

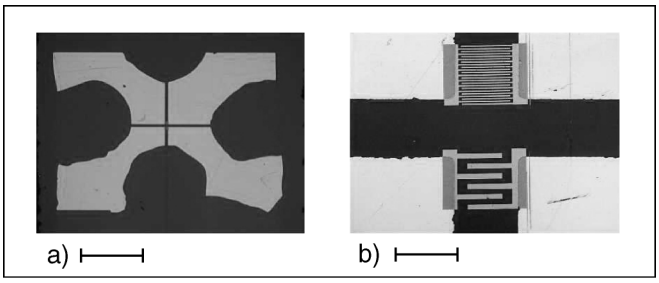

FIG. 3. (a) Double contact arrangement at 50× magnification showing bonding pads defined by optical lithography. Scale bar is 800 μm. (b) Same structure at 1000× magnification showing interdigitated contact arrangements defined by EBL. Scale bar is 40 μm. Separation between the contacts is 800 nm (top) and 3200 nm (bottom).

deposition time. Initial measurements were performed on samples with a single pair of contacts and Fig. 5(a) shows typical experimental data. At a clearly defined time during the deposition the cluster network becomes conducting over the length scale defined by the separation of the contacts and the current suddenly increases over several orders of magnitude. After the onset of conduction the current increases only slowly.

In principle the onset time can be related directly to the critical coverage $p_{\text{onset}}(L)$ through the deposition rate. Unfortunately it is very difficult to compare the deposition rates for depositions on single contact pairs due to nonuniformity in the cluster intensity laterally across the beam. The double contact pair arrangement shown in Fig. 3 eliminates that problem and has been used for all further experiments. The two contact pairs with different separations are defined very close together (40 μm apart), so that the cluster flux is the same for both, and the different onset times can directly be observed in the same run. For each sample, one pair of contacts was defined with a separation of 3200 nm and was used as a reference, thus calibrating the onset time obtained for the contacts with smaller separation. The ratio of the onset times gives immediately the ratio of the critical film thicknesses $d_C(L)/d_C(3200\ \text{nm})$. The data for a number of samples are plotted in Fig. 5(b), normalized to the critical film thickness for infinite contact separation $d_C(\infty)$ [18]. Since the surface coverage p is proportional to the mean film thickness, Eq. (2) can be rewritten as

$$d_C(L) - d_C(\infty) \propto L^{-z}, \tag{3}$$

which describes the experimental data very well with a fitted exponent $z = 0.6^{+0.3}_{-0.2}$. The experimental value for the exponent z is consistent with the value $1/\nu = 0.75$ predicted from our simulations for small σ_{min}.

The quantitative agreement between the experiments and simulations is a strong indication that the simple 2D site percolation model and the experimental system of bismuth clusters on a SiN surface belong to the same universality class [15]. In view of the obvious differences between the model system and the experimental one, this is in many ways a rather surprising result. That said, various other examples of universal behavior have been reported previously in very different types of experimental systems [16,19].

Although there have been several previous reports of ingenious experiments which allow the conductivity of a macroscopic percolating network to be measured (see, for example, [20–22]), and many measurements of percolating granular or nanocomposite films (see Ref. [23] and references therein), there has been no previous experimental

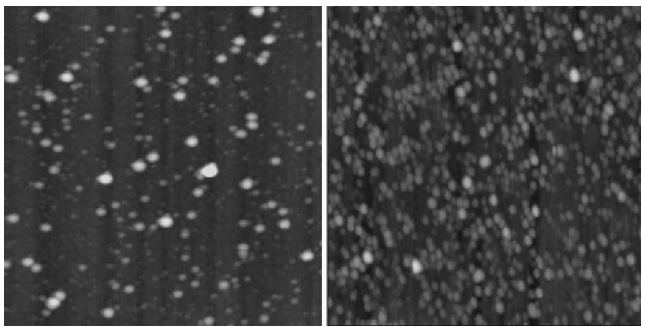

FIG. 4. AFM images of two large area cluster films with very different coverages. Each square has side 2 μm. The gray scale range represents a height of 50 nm. See text.

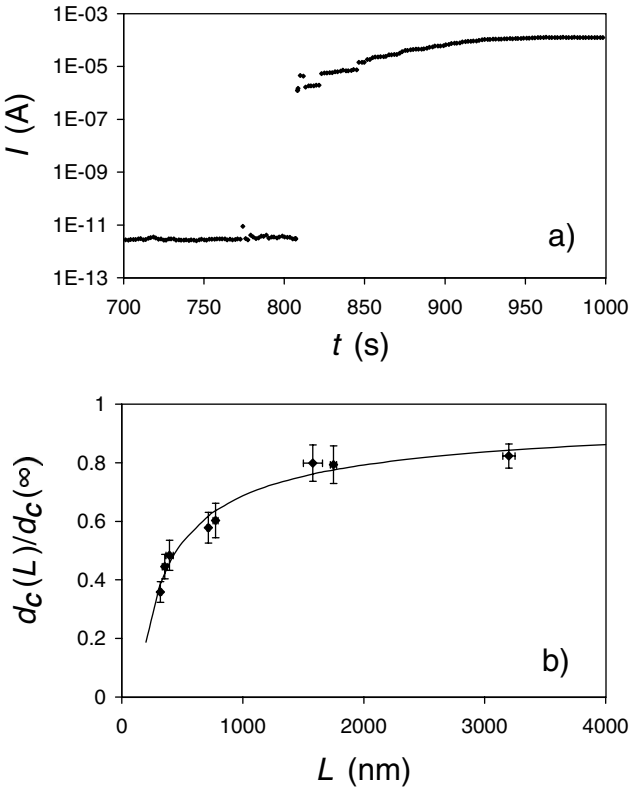

FIG. 5. (a) Current, I, as a function of time, t, for bismuth clusters deposited on a single set of contacts with separation 1600 nm. (b) Normalized critical film thickness $d_C(L)/d_C(\infty)$ as a function of system size L (contact separation). The solid line is a fit using Eq. (3); see text.

measurement of the shift of the percolation threshold with changing system size, or of the critical exponent for the correlation length, ν. Our choice of a rectangular system is critical in allowing us to address this issue.

The present work can be regarded as a direct experimental confirmation of the finite-size effects predicted by percolation theory. It also provides one of only a very few examples of a phase transition where the response to a variation of the system size is experimentally accessible [24].

The $I(t)$ data shown in Fig. 5(a) will be discussed in more detail elsewhere; however, the random steps in the current for $p > p_{\text{onset}}$ should be mentioned briefly. We believe that increases (decreases) in the current result from completion (destruction) of pathways in the film. This view is supported by $I(V)$ data for samples from runs in which deposition is stopped soon after the onset of conduction: these data show generally Ohmic behavior as well as sharp increases and decreases in the conductance of the film.

Finally, we highlight the fact that, for low surface coverages ($p \sim 0.25$), a connection between the contacts can be formed *only* by a wirelike chain of clusters. By using state-of-the-art electron beam lithography to fabricate contacts with spacings $\sim$10 nm, similar, but much smaller, nanowire structures should be achievable using clusters with diameters of a few nanometers. In general, devices fabricated from such small clusters would be necessary to observe memory effects. However, the present devices, which incorporate much larger ($\sim$60 nm) Bi clusters, may be interesting in their own right because the electron mean free paths and Fermi wavelengths in bismuth [25] are comparable to these cluster sizes.

Our method for the fabrication of cluster assembled nanostructures is attractive because it combines some of the advantages of both the "top-down" and "bottom-up" approaches to nanotechnology. In particular, the use of standard lithography techniques provides a simple and reliable method for the definition of the overall device geometry (and size), and the use of clusters offers the opportunity for nanometer scale minimum feature sizes (wire widths).

Cluster assembled devices may have a wide range of applications. In particular, the devices offer opportunities for simple chemical sensors (similar to those reported in, for example, [26]), and specific field effect transistor structures based on these devices may also be realizable.

Financial support from the DAAD (Germany) and the New Economy Research Fund (New Zealand) is gratefully acknowledged.

*Also at Fachbereich Physik, Universität Rostock, 18051 Rostock, Germany.

†Electronic address: S.Brown@phys.canterbury.ac.nz

[1] *Cluster Assembled Materials,* edited by K. Sattler (Trans Tech Publications, Zurich, 1996).
[2] *Metal Clusters at Surfaces,* edited by K. Meiwes-Broer (Springer, Berlin, 2000).
[3] *Cluster Beam Synthesis of Nanostructured Materials,* edited by P. Milani and S. Iannotta (Springer, Berlin, 1999).
[4] P. Melinon *et al.,* Int. J. Mod. Phys. B **9**, 339 (1995).
[5] W. Chen, H. Ahmed, and K. Nakazato, Appl. Phys. Lett. **66**, 3383 (1995).
[6] D. Klein, P. McEuen, J. B. Katari, R. Roth, and A. Alivisatos, Appl. Phys. Lett. **68**, 2574 (1996).
[7] D. Ralph, C. Black, and M. Tinkham, Phys. Rev. Lett. **78**, 4087 (1997).
[8] A. Bezryadin, C. Dekker, and G. Schmid, Appl. Phys. Lett. **71**, 1273 (1997).
[9] T. Sato, H. Ahmed, D. Brown, and B. Johnson, J. Appl. Phys. **82**, 696 (1997).
[10] C. Thelander, M. Magnusson, K. Deppert, L. Samuelson, P. R. Poulsen, J. Nygard, and J. Borggreen, Appl. Phys. Lett. **79**, 2106 (2001).
[11] *Finite-Size Scaling and Numerical Simulation of Statistical Systems,* edited by V. Privman (World Scientific, Singapore, 1990).
[12] S. Carroll, K. Seeger, and R. Palmer, Appl. Phys. Lett. **72**, 305 (1998).
[13] R. Barnett and U. Landman, Nature (London) **387**, 788 (1997).
[14] D. Stauffer, *Introduction to Percolation Theory* (Taylor and Francis, London, 1985).
[15] H. Stanley, Rev. Mod. Phys. **71**, S358 (1999).
[16] C. Back, C. Wursch, A. Vaterlaus, U. Ramsperger, U. Maier, and D. Pescia, Nature (London) **378**, 597 (1995).
[17] R. Monetti and E. Albano, Z. Phys. B **82**, 129 (1991).
[18] The equation $\gamma t_C(L)/t_C(3200\text{ nm}) - 1 \propto L^{-z}$ is fitted to the experimental data; $\gamma = t_C(3200\text{ nm})/t_C(\infty)$ and z are the fitted parameters; the plotted data are $t_C(L)/t_C(\infty) \equiv d_C(L)/d_C(\infty)$.
[19] S. Bramwell, P. Holdsworth, and J. Pinton, Nature (London) **396**, 552 (1998).
[20] B. Last and D. Thouless, Phys. Rev. Lett. **27**, 1719 (1971).
[21] M. Dubson and J. Garland, Phys. Rev. B **32**, 7621 (1985).
[22] A. Okazaki, K. Horibe, K. Maruyama, and S. Miyazima, Phys. Rev. E **61**, 6215 (2000).
[23] B. Raquet, M. Goran, N. Negre, J. Leotin, B. Aronzon, V. Rylkov, and E. Meilikhov, Phys. Rev. B **62**, 17 144 (2000).
[24] Others include the melting point of clusters, the onsets of ferromagnetism and superconductivity in small particles, and the 2D metal-insulator transition.
[25] M. Black, M. Padi, S. Cronin, Y. Lin, O. Rabin, T. McClure, G. Dresselhaus, P. Hagelstein, and M. Dresselhaus, Appl. Phys. Lett. **77**, 4142 (2000).
[26] C. Li, H. He, A. Bogozi, J. Bunch, and N. Tao, Appl. Phys. Lett. **76**, 1333 (2000).